metals

MDPI

Communication

Mechanical Property and Microstructure of Rolled 7075 Alloy under Hot Compression with Different Original Grains

Tuo Ye [1,2], Sawei Qiu [1,2], Erli Xia [1,2], Fang Luo [3], Wei Liu [1,2] and Yuanzhi Wu [1,2,*]

[1] School of Intelligent Manufacturing and Mechanical Engineering, Hunan Institute of Technology, Hengyang 421002, China; 2017001002@hnit.edu.cn (T.Y.); 2022001005@hnit.edu.cn (S.Q.); 2021001046@hnit.edu.cn (E.X.); 2015002039@hnit.edu.cn (W.L.)
[2] Research Institute of Automobile Parts Technology, Hunan Institute of Technology, Hengyang 421002, China
[3] School of Material Science and Engineering, Hunan Institute of Technology, Hengyang 421002, China; 20010340122@xs.hnit.edu.cn
* Correspondence: 2013001767@hnit.edu.cn

Abstract: The hot compression of rolled 7075 alloys with different heat treatments was performed. The temperature ranged from 200 to 400 °C, and the strain rate was 0.01 s^{-1}. The stress level decreases with the increasing temperature during compression, and the strength of the alloy in the original condition is higher than that of solution-treated (ST) alloy at the same deformation condition. The alloys with different heat treatments exhibit different anisotropic behaviors at 200 °C; the anisotropy for the alloys in both conditions becomes weaker with increasing temperature. Then, the corresponding microstructure was studied. The alloy's microstructure in its original condition consists of fiber grains; however, many equiaxed grains are found after solution treatment due to the recrystallization. The grains with different shapes lead to different anisotropic mechanical properties. For the alloys in both conditions, the density of the dislocation decreases with increasing temperature during compression, and a certain number of subgrains were found when deformed at 400 °C due to the higher driving force and a higher rate of atomic migration. Meanwhile, it is observed that the precipitates of the alloy become coarser during higher-temperature deformation. Dynamic softening is dominant in high-temperature deformation, decreasing stress during hot deformation.

Keywords: 7075 alloy; hot compression; mechanical property; microstructure

check for updates

Citation: Ye, T.; Qiu, S.; Xia, E.; Luo, F.; Liu, W.; Wu, Y. Mechanical Property and Microstructure of Rolled 7075 Alloy under Hot Compression with Different Original Grains. *Metals* **2023**, *13*, 1456. https://doi.org/10.3390/met13081456

Academic Editors: Ulrich Prahl and Hannu Hänninen

Received: 17 July 2023
Revised: 9 August 2023
Accepted: 11 August 2023
Published: 13 August 2023

Copyright: © 2023 by the authors. Licensee MDPI, Basel, Switzerland. This article is an open access article distributed under the terms and conditions of the Creative Commons Attribution (CC BY) license (https://creativecommons.org/licenses/by/4.0/).

1. Introduction

Heat treatable 7075 alloy is a traditional 7000 series aluminum alloy widely used in aircraft and vehicle industries due to its high strength, low density, attractive fracture toughness, and desirable corrosion resistance [1–3]. Also, the 7075 alloy exhibits excellent hot-forming ability, which contributes to broader use in structural applications [4–6]. The microstructure characteristics such as grain size and orientation, precipitates type and fraction, dislocations morphology, and density are mainly decided by hot deformation conditions [7–9]. Yang et al. [10] compressed the 7075 aluminum alloys with different grain sizes at high temperatures and found that the alloy with finer grains performed better in hot forming. Sun et al. [11] tested the as-extruded 7075 aluminum alloy at elevated temperature and concluded that only dynamic recovery was observed when the deforming temperature was below 350 °C; as the temperature exceeds 350 °C, dynamic recrystallization occurs. Meanwhile, the size of the recrystallization grain grows larger with increasing temperature. According to Taheri-Mandarjani et al. [12], when the temperature rises, the density of the second phase is found to decline; at the same time, the adverse effects of the particles on cavity nucleation and growth can be suppressed. Du et al. [13] tested the hot forming behavior of 7075 alloys at a range of 25–400 °C; it was found that the η phase is the main second phase, the size of the η phase increases with increasing temperature, and the coarsening of η phase leads to the weakening of mechanical properties. It is widely accepted

that the mechanical properties of metal material are highly related to its microstructure, which is greatly affected by the hot forming conditions [14–16]. Therefore, the studies of the deformation response and the associated microstructure evolution during compression at elevated temperatures are of great importance, contributing to a deeper understanding and better optimization of the forming process.

In practice, plastic forming is usually adopted to get the final shape of the products, during which the anisotropy of mechanical property often takes place [17–19]. In brief, the anisotropy can be explained by the fact that property values vary along different directions to the deformation axis [20]. It is proven that anisotropy may lead to unpredicted material mechanical properties. Yang et al. [21] studied the compression response of the extruded 7075 aluminum alloy bars with directions at 0°, 45°, and 90° to the extrusion direction. The results show that the 0° specimens have the highest flow stress, and the 45° specimens' flow stress is always the lowest. Hu et al. [22] found that the over-aged rolled 7050 aluminum alloy exhibit anisotropy in the elongation. The specimen parallel to the rolling direction exhibits the best elongation; however, the specimen with a 45° direction to the rolling direction owns the poorest elongation. It is well known that the crystallographic texture which forms during plastic deformation is mainly responsible for the anisotropy behavior. Also, it is reported that the microstructures formed during subsequent heat treatment, such as the grain shape, the particles, and the defects, may also lead to the anisotropy of aluminum alloys [23,24]. Hence, it is meaningful to study the anisotropy of 7075 aluminum alloy with different plastic deformation and heat treatment to make an accurate control and prediction of the material mechanical properties during forming.

Though the 7075 aluminum alloy was successfully used in industries, limited works on the relationship between anisotropic hot deformation behavior and the corresponding microstructure mechanism of this alloy have been found in open publications so far. This is significant for the manufacturing industry to better control and predict the final products. In the present study, the anisotropic hot deformation behavior and microstructure evolution of 7075 aluminum alloy were studied using a thermo-simulation machine, optical microscope (OM), electron back-scattered diffraction (EBSD), and transmission electron microscopy (TEM) technique. The aim is to reveal the relationship between flow stress response and microstructure evolution.

2. Experimental Procedures

The material is a rolling 7075-T6 alloy plate with a thickness of 10 mm; it is aging treated at 120 °C for 24 h after rolling and named as original (T6) condition. The chemical composition of this alloy is shown in Table 1.

Table 1. Chemical composition of 7075 aluminum alloy (mass fraction, %).

Composition	Cu	Mg	Fe	Si	Mn	Zn	Cr	Ti	Al
Content (%)	1.4	2.2	0.18	0.07	0.05	5.8	0.01	0.03	Bal.

The cylindrical specimens for the hot compression experiment have a diameter of 8 mm and a height of 12 mm. The compression samples were machined from the plate at angles of 0°, 45°, and 90° to the rolling direction (RD) (Figure 1). The received samples were solution-treated (ST) at 550 °C for 1 h and then cooled to room temperature in the water to get a different grain shape, named ST samples.

Hot compression was performed on a Gleeble 3500 thermal simulation machine (DSI, St. Paul, MN, USA) at temperatures of 200 °C, 300 °C, and 400 °C and strain rates of 0.01 s^{-1}. The hot compression parameters are shown in Figure 2. The sample ends were lubricated with Vaseline to minimize the friction effect. The specimens were heated to temperature during compression at a heating rate of 5 °C/s and held for 3 min to obtain a stable deformation temperature. The specimens were compressed to an engineering strain

of 0.75 and quenched with water for further comparative investigation of the deformation microstructure. The stress-strain curves were recorded by the computer automatically.

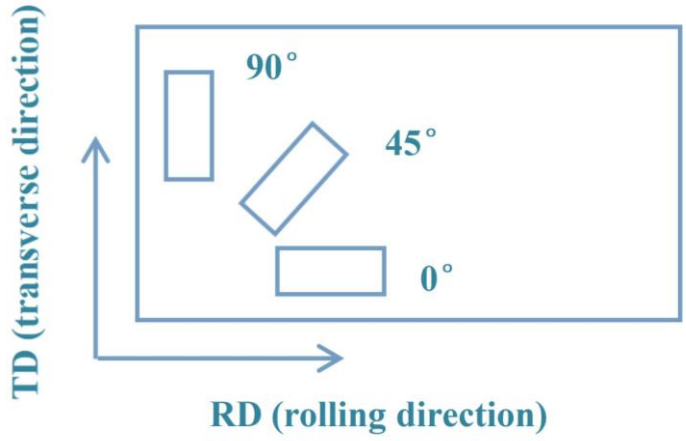


Figure 1. Schematic of the specimen direction.

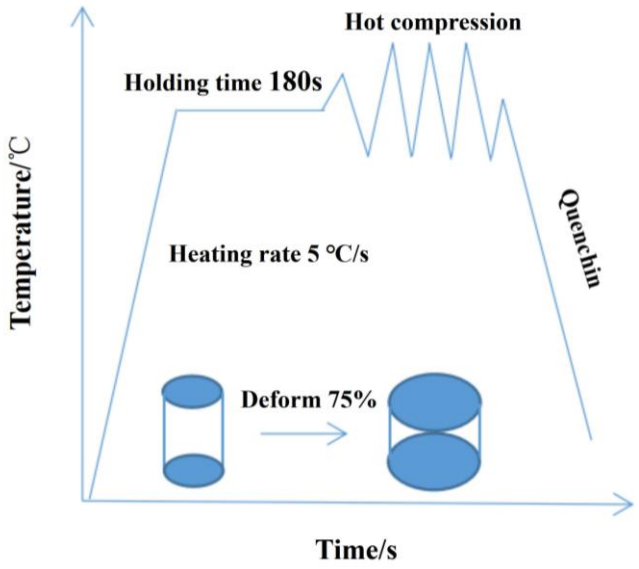


Figure 2. The parameters of hot compression.

The microstructure observation section for the specimens is paralleled to the compression axis. The compressed samples were polished, followed by anodizing in 5% HBF_4 solution, 20 V for 1–3 min, and the microstructures were observed under polarized light in an optical microscope (AX10, Zeiss, Oberkochen, Baden-Württemberg, Germany). After compression, the specimen surfaces parallel to the compressed axis were mechanically polished and electro-polished using 10% $HClO_4$ acids in alcohol. EBSD examination was conducted on a scanning electron microscope (EVO18, Zeiss, Oberkochen, Baden-Württemberg, Germany) with an accelerating voltage of 15 kV, and the data were analyzed using HKL Channel 5 software (Oxford Instruments, Eynsham Witney, Oxon, UK). Thin foil TEM samples were cut out from the cross-section of the original and compressed specimen. The discs were ground to a thickness of about 100 um, followed by electro-polishing in a double-jet unit operating at 10 V and −25 °C using a 30% nitric acid and 70% methanol solution. The electrolytic time is about 15 s. TEM investigations were performed on Tecnai G2 20 (FEI, Hillsboro, OR, USA) at an operating voltage of 300 kV.

3. Results and Discussion

3.1. Mechanical Properties

The engineering stress-strain curves during hot compression of rolled 7075 aluminum alloys are presented in Figure 3. In general, the engineering stresses rose rapidly with increasing strain and then held constant or decreased to some extent after reaching the peak values at different deformation conditions. During the compression, work hardening and dynamic softening will occur [25,26]. Both dynamic recovery and dynamic recrystallization are of great importance in deciding the microstructure evolution during hot compression, and the microstructure will also affect the mechanical property of the material [27,28]. It is clear that the hot compression was a competitive result of the dynamic softening and work hardening. At the beginning of the deformation, the rapid increase of dislocation density results in a dramatic increase in stress. However, as the deformation continues, dynamic softening, such as dynamic recovery or dynamic recrystallization, occurs, which can partially offset or even totally offset the strengthening effect of work hardening. As a result, the stress kept stable or decreased to some extent with the increasing engineering strain. It is clear that at the temperature of 300 °C, the engineering stresses of all condition samples rise to around 100 MPa, which is much lower than those at 200 °C. At the temperature of 400 °C, the flow stress is below 50 MPa. For both alloys deformed at 200 and 300 °C, the stress levels are low and keep stable during plastic deformation. With the increasing temperature, the diffusion ability of the atom increases, the activation energy to initiate the slip systems becomes lower, and more slip systems are activated, dynamic recovery and dynamic recrystallization are dominant. Also, the precipitate becomes coarse, contributing to decreasing stress levels [29].

Figure 4 shows the effects of temperature on the mechanical property of rolled 7075 alloys with different heat treatment conditions. The max stress decreases with increasing temperature for the alloy in both conditions. At the temperature of 200 °C, the stress of the original alloy is much higher than that of the ST alloy. This can attribute to the strengthening effect of the precipitates in the original alloy. During the deformation, the precipitates will impede the motion of the dislocation, which can enhance deformation resistance. As the temperature during compression increases to 400 °C, there seems to be no difference between the stress level of the alloys in both conditions.

It is found from Table 2 that the alloys with different heat treatments exhibit evident mechanical property anisotropy at the temperature of 200 °C. For the original alloy, the 0° samples have the highest stress level, and the stress level of the 45° samples is the lowest. For the solution-treated alloy, the stress level of 0° samples is the highest, and the 90° samples display the lowest stress level. It is reported that the fiber grains contribute to the anisotropic mechanical behavior; the sample that parallels the extrusion or rolling direction displays the highest flow stress [21]. Meanwhile, after high-temperature solution treatment, the grain size of the ST alloy becomes larger, recrystallization occurs, and the particles resolve into the matrix. Therefore, the preferred orientations change [30]. Also, it is worth noting that the mechanical property's anisotropy seems to be weaker with increasing temperature. At the temperature of 300 °C, the anisotropy of mechanical properties becomes less noticeable. However, there is no obvious anisotropy at the temperature of 400 °C. With the increasing temperature, the diffusion of the atom becomes more apparent; slip systems are easier to be activated, and the anisotropy for the alloys in both conditions becomes weak. Furthermore, at the temperature of 400 °C, the recrystallization is likely to weaken the anisotropy for both alloys.

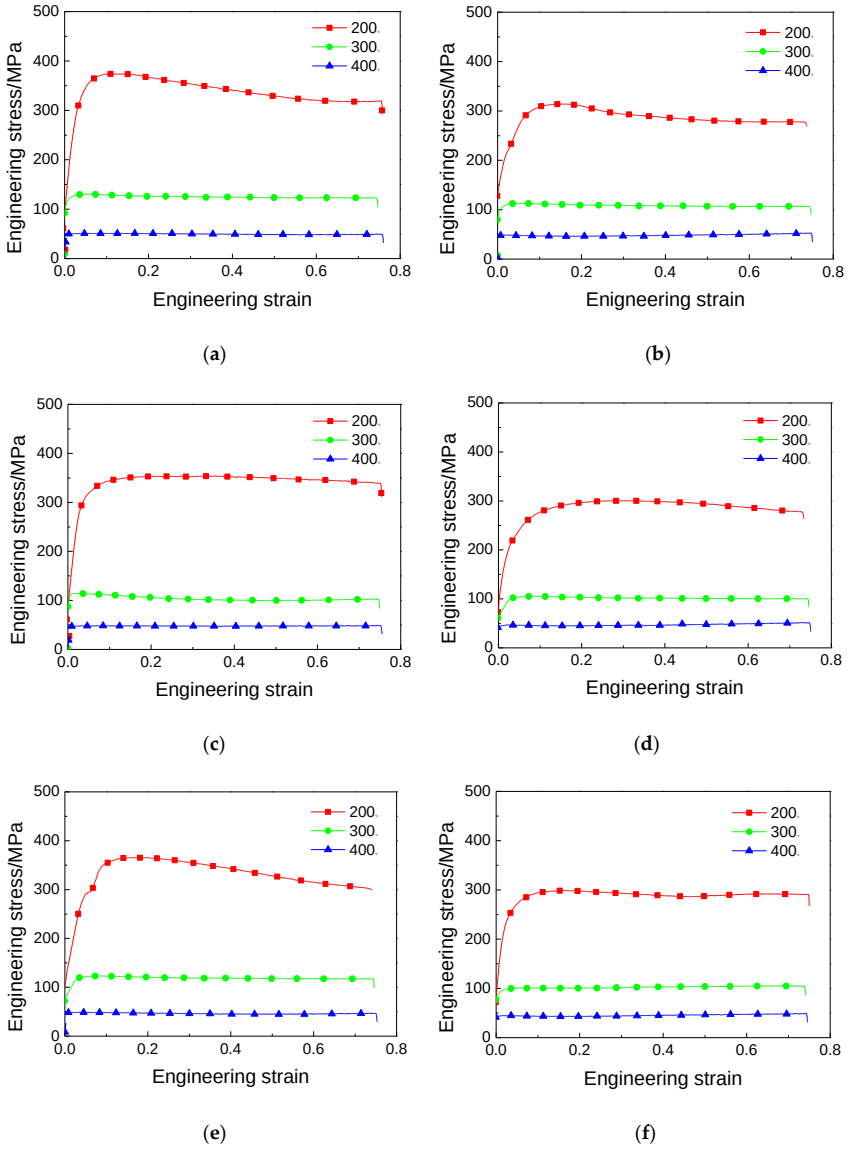


Figure 3. True stress-strain curves of the alloys with different heat treatment conditions: (**a**) original 0°, (**b**) original 45°, (**c**) original 90°, (**d**) ST 0°, (**e**) ST 45°, (**f**) ST 90°.

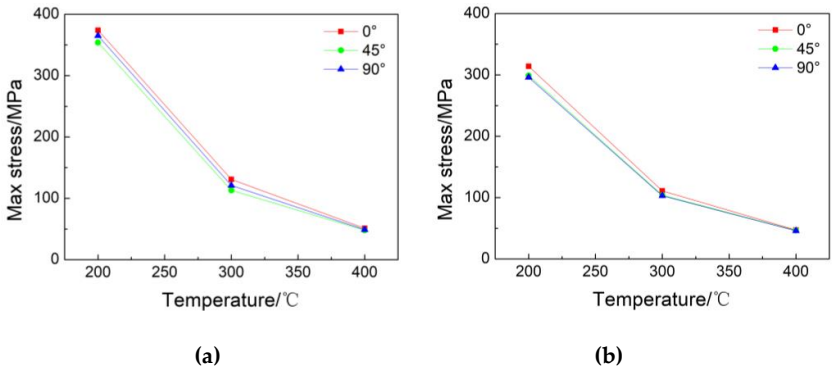


Figure 4. Effects of temperature on the mechanical property of rolled 7075 alloys: (**a**) original, (**b**) ST.

Table 2. The max stress of 7075 aluminum alloy with different conditions (MPa).

Temperature/°C	Original			Temperature/°C	ST		
	0°	45°	90°		0°	45°	90°
200	374	354	365	200	314	299	296
300	131	113	121	300	111	104	103
400	51	48	49	400	47	46	46

3.2. Microstructure Characterization

The mechanical property is highly related to the microstructure. Figure 5 is the grain structure of 7075 aluminum alloy with different heat treatments. The original alloy, as shown in Figure 6a, consists of fiber grains that result from the elongation of the grain after rolling deformation; the width of the fiber grain is between 20–30 μm. However, after solution treatment, the width of the grain becomes larger, the width of the grain is above 100 μm, and a fraction of equiaxed grains are observed due to the recrystallization (Figure 5b).

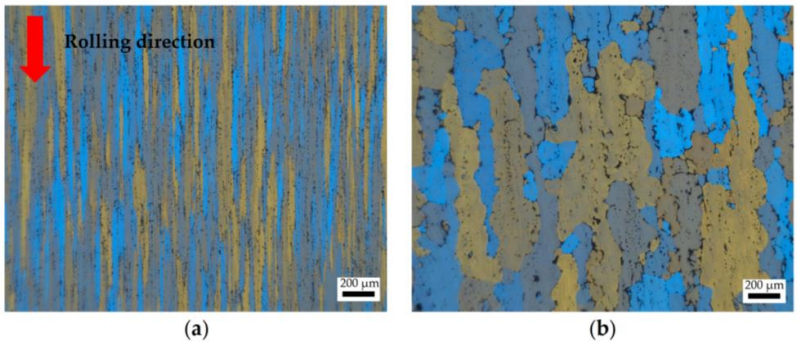


Figure 5. The grain structure of 7075 alloys with different heat treatments: (**a**) original, (**b**) ST.

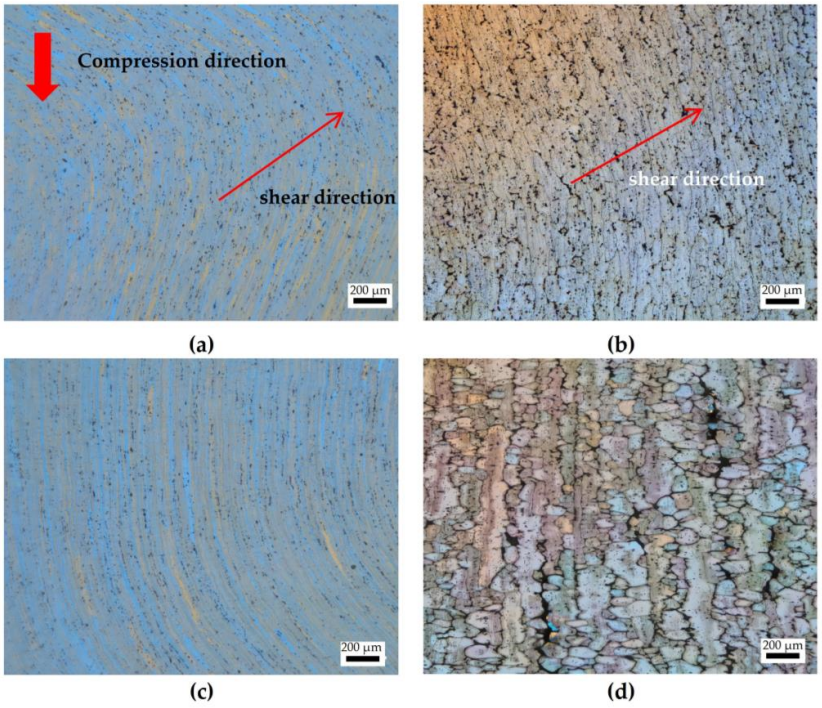


Figure 6. The grain structure of 7075 alloys 0° samples after deformation: (**a**) original 200 °C, (**b**) ST 200 °C, (**c**) original 400 °C, (**d**) ST 400 °C.

Figure 6 shows the grain structure of 7075 alloys after deformation. When deformed at 200 °C, the grains of alloys in both are distorted due to the shear stress (Figure 6a,b). The shear direction is 0° or 135° along the compression direction under the compression stress [31]. The original samples were distorted more severely than the ST samples. When deformed at 400 °C, the original alloy is less distorted than that deformed at 200 °C. Meanwhile, some fine grains are observed; this may be due to the recrystallization of 7075-T6 alloy deformed at elevated temperature [6,32] (Figure 6c). However, the ST alloy seems to deform homogeneously (Figure 6d). It is widely accepted that the recrystallization temperature of the alloy is taken as 0.5 Tm (melting temperature) [33]. For the 7075 aluminum alloy deformed at 400 °C, the temperature has exceeded the recrystallization temperature of the 7075 aluminum alloy, providing the condition for dynamic recrystallization. High temperature and large strain can supply more stored energy and act as a driving force to trigger dynamic recrystallization. The serration and breaking are observed along original grain boundaries, some equiaxed grains with large-angle grain boundaries are formed, but most are distributed at fiber grain boundaries [11,34]. Recrystallization occurs because of grain boundary migration; the grains merge and extend out after recrystallization, and the boundaries become straight [35]. Dynamic recrystallization can improve the plasticity of the aluminum and is beneficial for homogeneous deformation. Therefore, it is worth considering the recrystallization behavior during high-temperature deformation.

From TEM images, we can find that precipitates with small sizes are uniformly distributed in the original alloy (Figure 7a); the main precipitate in 7075-T6 is fine η′ (plate-shaped) and coarse η phase (needle-shaped) [36–39]. Meanwhile, the elongated grains resulting from severe rolling deformation were detected. However, no obvious precipitate was found in the solution-treated 7075 alloys before compression (Figure 7b), and only a small fraction of dislocation lines were observed. During high-temperature solution treatment, the density of vacancy decreases greatly, and the dislocations inside the cell slip towards the cell wall; the heterologous dislocations begin to annihilate. Therefore, the dislocation density decreases to some extent. During compression deformation, the precipitates in the alloy matrix will pin the dislocations and impede the migration of subgrains [40]. On the other hand, the high density of precipitate can restrict the movement of dislocations and high-angle boundaries. Therefore, the process of recrystallization then requires higher temperatures to complete; the presence of precipitate can effectively improve the recrystallization temperature of the alloy, which slows down the softening effect [41,42]. Therefore, the higher max stresses of the original alloy, as shown in Figure 3, can be explained. Also, during high-temperature solution treatment, the high density of dislocation decreased significantly, and the fiber grain grew larger, resulting in a lower stress level of ST alloy.

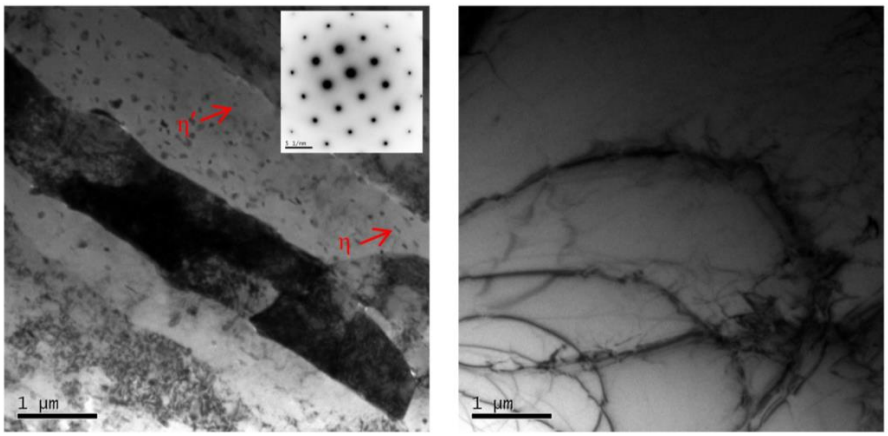


Figure 7. The TEM images of 7075 alloy 0° samples with different heat treatments: (**a**) original, (**b**) ST.

Figure 8 shows the TEM observation of 7075 in original and ST conditions compressed with different deformation parameters. It can be seen from Figure 8a,b that when the alloys are deformed at 200 °C, a high density of dislocations is found in the samples with different heat treatment conditions. In the original sample, several precipitates with small sizes are detected, and the length of the phase is less than 100 nm. However, in the solution-treated sample, no precipitate is observed. When deformed at 400 °C, it is clear that the density of dislocations decreases with increasing temperature. Meanwhile, a certain number of subgrains are found in Figure 8c,d; at higher deformation temperatures, the higher driving force can accelerate the dislocation movement and form the boundaries of a polygonized subgrain structure [43]. In addition, the sufficient migration of atoms and dislocations at higher temperatures can also result in subgrain growth. Moreover, a great number of precipitates with large sizes appear due to the coarsening of precipitate [44,45]. The length of the phase is between 150–200 nm. The increase in phase size will weaken the strengthening effect and decrease the mechanical properties of the alloy [13].

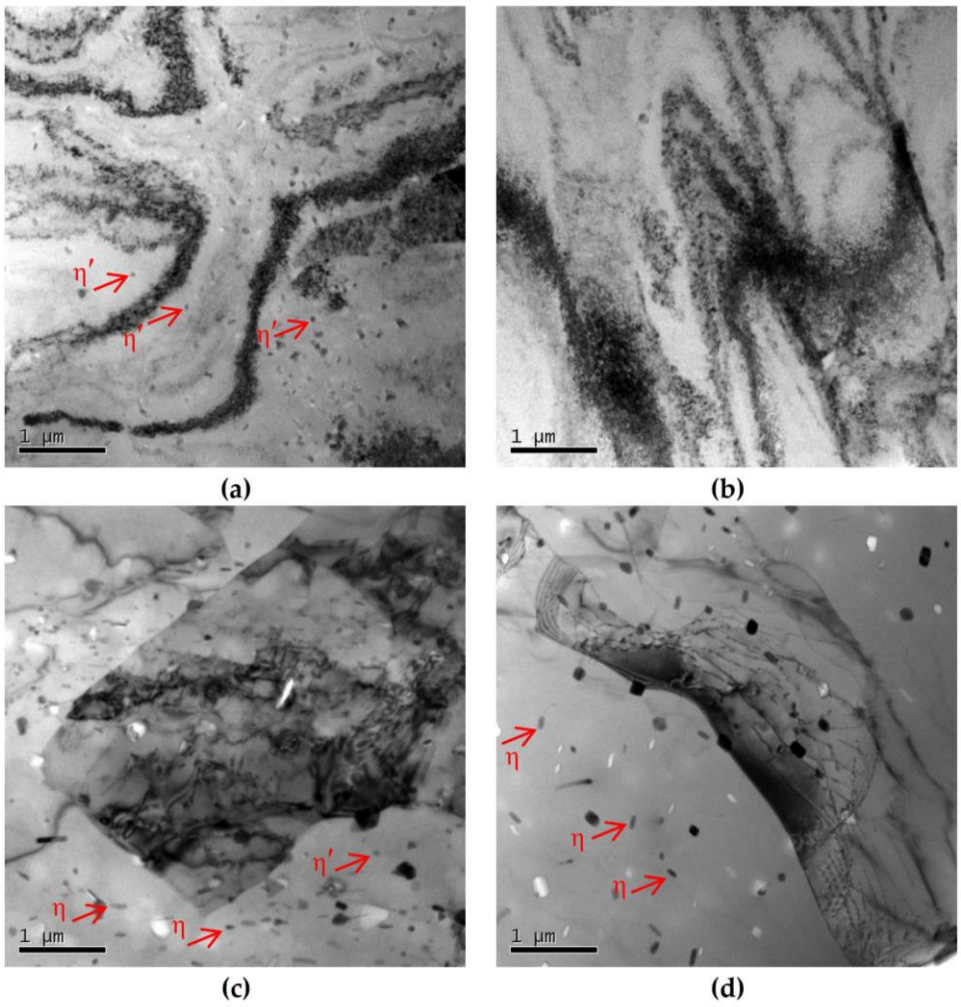


Figure 8. The TEM images of 7075 alloy 0° samples after compression: (**a**) original compressed at 200 °C, (**b**) ST compressed at 200 °C, (**c**) original compressed at 400 °C, (**d**) ST compressed at 400 °C.

4. Conclusions

The hot compression behavior and corresponding microstructure evolution of a rolled 7075 aluminum alloy with different grain shapes have been investigated. The following are the conclusions:

1. The flow stress decreases significantly with increasing temperature during compression. The flow stress rises rapidly with the increasing strain and reaches a maximum

value, then gradually decreases before reaching a stable value; the compression process of the alloy is a competing result of work hardening and dynamic softening.

2. The alloys in both conditions display evident anisotropic mechanical properties at 200 °C. For the original alloy, the 0° sample has the highest stress, and the 45° sample exhibits the lowest stress. For solution-treated alloy, the stress of the 0° sample is the highest, and the 90° sample owns the lowest stress. The anisotropy becomes less noticeable at 300 °C. There is no obvious anisotropy at 400 °C for both alloys.
3. At 200 °C, the stress of the original alloy is much higher than that of the solution-treated alloy at the same compression condition. The small and uniformly distributed precipitates can enhance the stress level by impeding the motion of dislocation and the slide of subgrains.
4. For the 7075 alloys in both conditions, with increasing temperature, the density of the dislocation decreases. The structure of subgrains was found when deformed at 400 °C due to the higher driving force and a higher rate of atomic migration. Meanwhile, the coarsening of the precipitate is found.

Author Contributions: Conceptualization, T.Y.; Methodology, Y.W. and W.L.; Data curation, F.L. and S.Q.; Validation, S.Q. and W.L.; Visualization E.X. and F.L.; Formal analysis, T.Y.; Funding acquisition, Y.W.; Investigation, T.Y.; Resources, E.X. and W.L.; Supervision Y.W.; Writing-original draft, T.Y.; Writing-review and editing, E.X. and Y.W. All authors have read and agreed to the published version of the manuscript.

Funding: The research described in this paper was supported by Scientific Research Fund of Hunan Provincial Education Department of China (22A0626, 22B0867), Natural Science Foundation of Hunan Province (2022JJ50146), Science and Technology Innovation Program of Hunan Province (2021RC1008).

Institutional Review Board Statement: Not applicable.

Data Availability Statement: Not applicable.

Conflicts of Interest: The authors declare no conflict of interest.

References

1. Chambrin, N.; Dalverny, O.; Descamps-Mandine, A.; Cloue, J.M.; Brucelle, O.; Alexis, J. Influence of heat treatments on microstructure and hardness of a high-strength Al-Zn-Mg-Cu-Zr alloy processed by laser powder bed fusion. *Metals* **2023**, *13*, 1173. [CrossRef]
2. Lin, R.; Liu, B.; Zhang, J.; Zhang, S. Microstructure evolution and properties of 7075 aluminum alloy recycled from scrap aircraft aluminum alloys. *J. Mater. Res. Technol.* **2022**, *19*, 354–367. [CrossRef]
3. Ji, H.C.; Qiao, J.H.; Kang, N.Z.; Wang, X.L.; Huang, J.H. Optimization of hot extrusion process parameters for 7075 aluminum alloy rims based on HyperXtrude. *J. Mater. Res. Technol.* **2023**, *25*, 4913–4928. [CrossRef]
4. Liu, M.; Shan, Z.; Li, X.; Zang, Y. Hot tensile deformation behavior and microstructure evolution of 7075 aluminum alloy sheet. *J. Mater. Res. Technol.* **2023**, *24*, 724–736. [CrossRef]
5. Geng, H.C.; Wang, Y.L.; Zhu, B.; Wang, Z.J.; Zhang, Y.S. Effect of solution treatment time on plasticity and ductile fracture of 7075 aluminum alloy sheet in hot stamping process. *T. Nonferrous Met. Soc.* **2022**, *32*, 3516–3533. [CrossRef]
6. El-Shenawy, E.; Farahat, A.I.Z.; Ragab, A.E.; Elsayed, A.; Reda, R. Flow behavior and mechanical properties of multi-pass thermomechanically processed 7075 Al-alloy. *Metals* **2023**, *13*, 1158. [CrossRef]
7. Jiang, F.; Masumura, T.; Hirata, K.; Tsuchiyama, T.; Takaki, S. A new diffraction line profile breadth analysis approach for evaluating plastic lattice strain anisotropy in cold-worked nickel under various strain paths. *Int. J. Plast.* **2019**, *112*, 89–107. [CrossRef]
8. Zhu, S.Y.; Zhao, M.; Mao, J.; Liang, S.Y. Study on hot deformation behavior and texture evolution of aluminum alloy 7075 based on visco-plastic self-consistent model. *Metals* **2022**, *12*, 1648. [CrossRef]
9. Jiang, F.; Zhang, H.; Li, L.; Chen, J. The kinetics of dynamic and static softening during multistage hot deformation of 7150 aluminum alloy. *Mater. Sci. Eng. A* **2012**, *552*, 269–275. [CrossRef]
10. Yang, Y.; Zhang, Z.; Li, X.; Wang, Q.; Zhang, Y. The effects of grain size on the hot deformation and processing map for 7075 aluminum alloy. *Mater. Des.* **2013**, *51*, 592–597. [CrossRef]
11. Sun, Z.C.; Zheng, L.S.; Yang, H. Softening mechanism and microstructure evolution of as-extruded 7075 aluminum alloy during hot deformation. *Mater. Charact.* **2014**, *90*, 71–80. [CrossRef]

12. Taheri-Mandarjani, M.; Zarei-Hanzaki, A.; Abedi, H.R. Hot ductility behavior of an extruded 7075 aluminum alloy. *Mater. Sci. Eng. A* **2015**, *637*, 107–122. [CrossRef]
13. Du, Z.H.; Deng, Z.S.; Cui, X.H.; Xiao, A. Deformation behavior and properties of 7075 aluminum alloy under electromagnetic hot forming. *Materials* **2021**, *14*, 4954. [CrossRef]
14. Li, H.B.; Chen, M.S.; Tian, Y.Q.; Chen, L.S.; Chen, L.Q. Ultra-fine-grained ferrite prepared from dynamic reversal austenite during warm deformation. *Acta Metall. Sin.* **2020**, *33*, 290–298. [CrossRef]
15. Zhu, B.; Liu, X.; Xie, C.; Su, J.; Guo, P.; Tang, C.; Liu, W. Unveiling the underlying mechanism of forming edge cracks upon high strain-rate rolling of magnesium alloy. *J. Mater. Sci. Sci Technol.* **2020**, *50*, 59–65. [CrossRef]
16. Jiang, F.; Zurob, H.S.; Purdy, G.R.; Zhang, H. Characterizing precipitate evolution of an Al-Zn-Mg-Cu-based commercial alloy during artificial aging and non-isothermal heat treatments by in situ electrical resistivity monitoring. *Mater. Charact.* **2016**, *117*, 47–56. [CrossRef]
17. Moghaddam, M.; Zarei-Hanzaki, A.; Pishbin, M.H.; Shafieizad, A.H.; Oliveira, V.B. Characterization of the microstructure, texture and mechanical properties of 7075 aluminum alloy in early stage of severe plastic deformation. *Mater. Charact.* **2016**, *119*, 137–147. [CrossRef]
18. Ma, J.; Wang, Q.; Zhang, T.; Cao, H.; Yang, Y.; Zhang, Z. Effect of natural aging time on tensile and fatigue anisotropy of extruded 7075 Al alloy. *J. Mater. Res. Technol.* **2022**, *18*, 4683–4697. [CrossRef]
19. Senthil, K.; Iqbal, M.A.; Chandel, P.S.; Gupta, N.K. Study of the constitutive behavior of 7075-T651 aluminum alloy. *Int. J. Impact Eng.* **2017**, *108*, 171–190. [CrossRef]
20. Singh, R.K.; Singh, A.K.; Prasad, N.E. Texture and mechanical property anisotropy in an Al-Mg-Si-Cu alloy. *Mater. Sci. Eng. A* **2000**, *277*, 114–122. [CrossRef]
21. Yang, Y.; Xie, Z.P.; Zhang, Z.; Li, X.; Wang, Q.; Zhang, Y. Processing maps for hot deformation of the extruded 7075 aluminum alloy bar, Anisotropy of hot workability. *Mater. Sci. Eng. A* **2014**, *615*, 183–190. [CrossRef]
22. Hu, H.; Wang, X. Effect of heat treatment on the in-plane anisotropy of as-rolled 7050 aluminum alloy. *Metals* **2016**, *6*, 79. [CrossRef]
23. Choi, S.H.; Brem, J.C.; Barlat, F.; Oh, K.H. Macroscopic anisotropy in AA5019A sheets. *Acta Mater.* **2000**, *48*, 1853–1863. [CrossRef]
24. Choi, S.H.; Barlat, F.; Liu, J. Effect of precipitates on plastic anisotropy for polycrystalline aluminum alloys. *Metall. Mater. Trans. A* **2001**, *32*, 2239–2247. [CrossRef]
25. Wu, H.; Wen, S.P.; Huang, H.; Wu, X.L.; Gao, K.Y.; Wang, W.; Nie, Z.R. Hot deformation behavior and constitutive equation of a new type Al-Zn-Mg-Er-Zr alloy during isothermal compression. *Mater. Sci. Eng. A* **2016**, *651*, 415–424. [CrossRef]
26. Yang, H.B.; Bu, H.Y.; Li, M.N.; Lu, X. Prediction of flow stress of annealed 7075 Al alloy in hot deformation using strain-compensated arrhenius and neural network models. *Materials* **2021**, *14*, 5986. [CrossRef]
27. Jiang, F.; Zhang, H.; Su, J.; Sun, Y. Constitutive characteristics and microstructure evolution of 7150 aluminum alloy during isothermal and non-isothermal multistage hot compression. *Mater. Sci. Eng. A* **2015**, *636*, 459–469. [CrossRef]
28. Tang, J.; Wang, J.H.; Teng, J.; Wang, G.; Fu, D.F.; Zhang, H.; Jiang, F.L. Effect of Zn content on the dynamic softening of Al-Zn-Mg-Cu alloys during hot compression deformation. *Vacuum* **2021**, *184*, 109941. [CrossRef]
29. Yang, W.P.; Li, J.R.; Liu, S.Z.; Shi, Z.X.; Zhao, J.Q.; Wang, X.G. Orientation dependence of transverse tensile properties of nickel-based third generation single crystal superalloy DD9 from 760 to 1100 °C. *T. Nonferr. Metal Soc.* **2019**, *29*, 558–568. [CrossRef]
30. Bois-Brochu, A.; Blais, C.; Goma, F.A.T.; Larouche, D.; Boselli, J.; Brochu, M. Characterization of Al–Li 2099 extrusions and the influence of fiber texture on the anisotropy of static mechanical properties. *Mater. Sci. Eng. A* **2014**, *597*, 62–69. [CrossRef]
31. Ye, T.; Li, L.X.; Liu, X.; Liu, W.H.; Guo, P.C.; Tang, X. Anisotropic deformation behavior of as-extruded 6063-T4 alloy under dynamic impact loading. *Mater. Sci. Eng. A* **2016**, *666*, 149–155. [CrossRef]
32. Chakraborty, P.; Singha, M.K.; Tiwari, V. Anisotropic mechanical response of AA7475-T7351 alloy at different loading rates and temperatures. *Thin Wall Struct.* **2023**, *188*, 110842. [CrossRef]
33. Li, D.H.; Yang, Y.; Xu, T.; Zheng, H.G.; Zhu, Q.S.; Zhang, Q.M. Observation of the microstructure in the adiabatic shear band of 7075 aluminum alloy. *Mater. Sci. Eng. A* **2010**, *527*, 3529–3535. [CrossRef]
34. Han, W.; Zhang, H.M.; Cui, Z.S.; Chen, Z.; Chen, D. Compressive response and microstructural evolution of in-situ TiB2 particle-reinforced 7075 aluminum matrix composite. *T. Nonferrous Metal Soc.* **2021**, *31*, 1235–1248.
35. Liu, C.; Liu, Y.L.; Ma, L.Y.; Yi, J.H. Effects of solution treatment on microstructure and high-cycle fatigue properties of 7075 aluminum alloy. *Metals* **2017**, *7*, 193. [CrossRef]
36. Luo, J.; Luo, H.Y.; Zhao, T.S.; Wang, R.Z. Effect of magnetic field on dislocation morphology and precipitation behaviour in ultrafine-grained 7075 aluminium alloy. *J. Mater. Sci. Technol.* **2021**, *93*, 128–146. [CrossRef]
37. Yin, X.L.; Deng, W.J.; Zou, Y.H.; Zhang, J.Y. Ultrafine grained Al 7075 alloy fabricated by cryogenic temperature large strain extrusion machining combined with aging treatment. *Mater. Sci. Eng. A* **2019**, *762*, 138106. [CrossRef]
38. Zhang, P.; Liu, Z.H.; Liu, J.L.; Yu, J.; Mai, Q.Q.; Yue, X.J. Effect of aging plus cryogenic treatment on the machinability of 7075 aluminum alloy. *Vacuum* **2023**, *208*, 111692. [CrossRef]
39. Feng, B.; Gu, B.; Li, S.H. Cryogenic deformation behavior and failure mechanism of AA7075 alloy sheets tempered at different conditions. *Mater. Sci. Eng. A* **2022**, *848*, 143396. [CrossRef]

40. Zhang, H.; Jin, N.P.; Chen, J.H. Hot deformation behavior of Al-Zn-Mg-Cu-Zr aluminum alloys during compression at elevated temperature. *J. Trans. Nonferrous Met. Soc. China* **2011**, *21*, 437–442. [CrossRef]
41. Leng, J.F.; Ren, B.H.; Zhou, Q.B.; Zhao, J.W. Effect of Sc and Zr on recrystallization behavior of 7075 aluminum alloy. *T. Nonferr. Metal Soc.* **2021**, *31*, 2545–2557. [CrossRef]
42. Li, H.Y.; Gao, Z.H.; Yin, H.; Jiang, H.F.; Su, X.J.; Bin, J. Effects of Er and Zr additions on precipitation and recrystallization of pure aluminum. *Scripta Mater.* **2013**, *68*, 59–62. [CrossRef]
43. Wu, H.; Wen, S.P.; Huang, H.; Gao, K.Y.; Wu, X.L.; Wang, W.; Nie, Z.R. Hot deformation behavior and processing map of a new type Al-Zn-Mg-Er-Zr alloy. *J. Alloys Compd.* **2016**, *685*, 869–880. [CrossRef]
44. Shojaei, K.; Sajadifar, S.V.; Yapici, G.G. On the mechanical behavior of cold deformed aluminum 7075 alloy at elevated temperatures. *Mater. Sci. Eng. A* **2016**, *670*, 81–89. [CrossRef]
45. Lin, Y.C.; Jiang, Y.Q.; Chen, X.M.; Wen, D.X.; Zhou, H.M. Effect of creep-aging on precipitates of 7075 aluminum alloy. *Mater. Sci. Eng. A* **2013**, *588*, 347–356. [CrossRef]

Disclaimer/Publisher's Note: The statements, opinions and data contained in all publications are solely those of the individual author(s) and contributor(s) and not of MDPI and/or the editor(s). MDPI and/or the editor(s) disclaim responsibility for any injury to people or property resulting from any ideas, methods, instructions or products referred to in the content.